

## Electrochemical and photoelectrochemical studies of C. I. Acid Orange 52 oxidation

Rafał Salata<sup>1</sup>, Ewa Chrześcijańska<sup>2</sup>, Jolanta Sokołowska<sup>1,\*</sup>

<sup>1</sup> Institute of Polymer and Dye Technology, Lodz University of Technology, Stefanowskiego 12/16, 90-924 Lodz, Poland

<sup>2</sup> Institute of General and Ecological Chemistry, Lodz University of Technology, Żeromskiego 116, 90-924 Lodz, Poland

\*E-mail: [jsokolow@p.lodz.pl](mailto:jsokolow@p.lodz.pl)

Received: 2 January 2019 / Accepted: 1 March 2019 / Published: 10 April 2019

---

Basic electrochemistry (oxidation) of C. I. Acid Orange 52 at a platinum electrode was investigated. The electrochemical and photoelectrochemical oxidation of C. I. Acid Orange 52 were also conducted using a titanium electrode coated with a mixture of TiO<sub>2</sub>/RuO<sub>2</sub>. The conversion of the dye was observed as a change in absorbance ( $\eta_{\text{Abs}}$ ) at  $\lambda_{\text{max}}$ , total organic carbon ( $\eta_{\text{TOC}}$ ) and chemical oxygen demand ( $\eta_{\text{COD}}$ ). Quantum chemical calculations were conducted using the B3LYP/6-31G+ density functional theory (DFT) and AM1 method with HyperChem software to predict the primary oxidation products.

---

**Keywords:** electrochemical oxidation, photoelectrochemical oxidation, quantum chemical calculation, DFT.

### 1. INTRODUCTION

Azo dyes are the most frequently used colorants. They are used extensively in the textile, cosmetics, paper, leather, drug and food industries. The reason for their common application is their low price, simplicity of synthesis and wide gamut of colours. The particular application of the dyes makes them designed to be adherent, long lasting, and, most importantly, highly resistant to many factors, such as pH, temperature, abrasion, light, water and other chemicals. Textile dyes are especially dangerous to the environment because up to 30% of them remain in the spent dye-bath [1, 2]. These effluents have a very strong colour that causes not only aesthetic problems but also harm to aquatic organisms, due to the decomposition of the colorants to potentially toxic, mutagenic and carcinogenic compounds. Since these dyes exhibit relatively low biodegradability [3], currently used degradation methods such as adsorption, flocculation and coagulation are not fully sufficient for their removal.

Electrochemical oxidation of organic waste has received a great deal of attention due to its attractive characteristics of energy efficiency, possibility of automation and versatility [4]. The electrochemical destruction of organic compounds may be achieved by direct anode oxidation or/and by indirect oxidation by strong oxidants generated at the anode, such as hydroxyl radicals. Previously, many different anodes, such as lead, platinum, graphite and lead dioxide, were used. Additionally, titanium anodes coated with metal oxides (titanium or ruthenium) were found to be very effective [5, 6]. However, there are still new approaches to improve the decolouration of textile wastewater containing water-soluble dyes. Most of these studies relate to C. I. Acid Orange 52. For example, electrochemical studies employing Pt-Bi/C [7], Ti/Ir-Pb, Ti/Ir-Sn, Ti/Ru-Pb, Ti/Pt-Pd and Ti/RuO<sub>2</sub> [8] as anode materials and photoelectrocatalytic studies using Yb/WO<sub>3</sub> [9] were reported recently. The electrochemical oxidation of azo dyes leads to short-chain carboxylic acids as final products [10-12]. Malic, succinic and acetic acids resulting from cleavage of the benzene rings of the azo dye [11-13] were detected, along with oxalic and oxamic acids. The same results were found by means of gas chromatography, mass spectrometry and ion-exclusion high-performance liquid chromatography of methyl orange during its electrochemical oxidation at a Ti/Ir-Pb anode [8]. Although the degradation of C. I. Acid Orange 52 has been extensively studied for years using very sophisticated methods, data concerning its mineralisation to water and carbon dioxide, based on TOC or COD measurements, have been reported in only a few papers.

The aim of this paper is an extensive study of the basic electrochemistry (electrooxidation) of C. I. Acid Orange 52 (Figure 1) at different anode materials and the evaluation of the optimal conditions to achieve the highest mineralisation of the dye by the combination of electrochemical and photochemical techniques. In electrochemical and photoelectrochemical methods, titanium electrodes coated with a mixture of titanium and ruthenium oxides are used. The primary dye oxidation products are proposed based on quantum chemical calculations (AM1 method with HyperChem software and the B3LYP/6-31G+ density functional theory (DFT)).

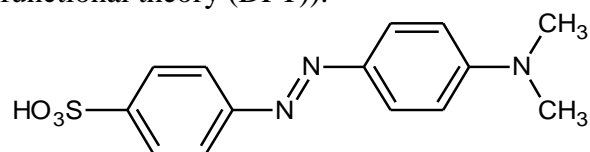


**Figure 1.** C. I. Acid Orange 52 (methyl orange, MO).

## 2. EXPERIMENTAL

### 2.1. Reagents and materials

C. I. Acid Orange 52 was purchased from Sigma-Aldrich (Poznan, Poland). The concentration of C. I. Acid Orange 52 solutions varied in the range from 0.25 to 2.0 mmol dm<sup>-3</sup>. Aqueous solutions were prepared by dissolving the substrate in 0.1 mol NaClO<sub>4</sub> (Fluka). In experiments, doubly distilled water was used. H<sub>2</sub>SO<sub>4</sub> was purchased from Chempur, Poland. Ag<sub>2</sub>SO<sub>4</sub>, K<sub>2</sub>Cr<sub>2</sub>O<sub>7</sub> and Fe(NH<sub>4</sub>)<sub>2</sub>(SO<sub>4</sub>)<sub>2</sub> were purchased from POCh Gliwice, Poland. All reagents, with the exception of the dye, were of analytical grade.

## 2.2. Basic electrochemistry

The kinetic parameters were determined using cyclic voltammetry (CV) [14, 15] and differential pulse voltammetry (DPV) methods. CV and DPV were recorded in the potential range from 0 to 1.1 or 1.2 V. CV was recorded at various scan rates (0.01 to 0.5 V s<sup>-1</sup>). DPV was recorded over the same potential range with a modulation amplitude of 25 mV, and a pulse width of 50 ms (scan rate 0.01 V s<sup>-1</sup>). The measurements were conducted in an Autolab PGSTAT 30 Electrochemical Analyser (EcoChemie, Netherlands). A three-electrode cell was used in all experiments. A titanium electrode coated with TiO<sub>2</sub>/RuO<sub>2</sub> (97%/3% or 70%/30%) was used as the anode (obtained from the Department of Inorganic Chemistry and Technology of Silesian Technical University), and a platinum electrode was used as the working electrode (geometric surface area of 0.5 cm<sup>2</sup>). The cathode was a platinum electrode. The potential of the working electrode was measured using a saturated calomel electrode (SCE). Before and during measurements, the solutions were deoxidised by purging with argon. All experiments were carried out at room temperature. The peak potential (E<sub>p</sub>), the potential at which the current is half of the peak value (E<sub>p/2</sub>) and the half-wave potential (E<sub>1/2</sub>) for the first step of C. I. Acid Orange 52 electrooxidation were determined from voltammograms. The anodic transition coefficient (β<sub>nβ</sub>) and heterogeneous rate constant (k<sub>bh</sub>) at the half-wave potential (E<sub>1/2</sub>) were calculated from the equations presented in the literature [15].

## 2.3. Electrolytic and photoelectrolytic degradation experiments

Preparative oxidation of the dyes was carried out in an electrochemical quartz cell with undivided electrode compartments under galvanostatic conditions. A current intensity of 0.4 A was used at the electrode surface of 20 cm<sup>2</sup>, which corresponds to a current density of 2.0 x 10<sup>-2</sup> A cm<sup>-2</sup>. Photoelectrochemical oxidation of the dyes was carried out in the same electrochemical cell placed in the photochemical reactor (Rayonet RPR-200, Southern New England Ultraviolet Company) equipped with eight lamps emitting radiation at 254 nm (radiation intensity 11.3 mW cm<sup>-2</sup>) and 300 nm (radiation intensity 6.4 mW cm<sup>-2</sup>) for 1.5 h.

The conversion of the dye presented as a change in absorbance (η<sub>Abs</sub>) at λ<sub>max</sub>, total organic carbon (η<sub>TOC</sub>) and chemical oxygen demand (η<sub>COD</sub>) were calculated as follows:

$$\eta_{Abs} = \frac{A_0 - A_t}{A_0} \times 100\% \quad (1)$$

$$\eta_{TOC} = \frac{TOC_0 - TOC_t}{TOC_0} \times 100\% \quad (2)$$

$$\eta_{COD} = \frac{COD_0 - COD_t}{COD_0} \times 100\% \quad (3)$$

where A<sub>0</sub>, TOC<sub>0</sub> and COD<sub>0</sub> are the initial values of the measured parameters and A<sub>t</sub>, TOC<sub>t</sub> and COD<sub>t</sub> denote their values at time t.

The absorption spectra were recorded using a Jasco V-670 spectrophotometer (Jasco, Japan). TOC was analysed with a TOC 5050 A Shimadzu Total Organic Carbon Analyser (Japan). COD was determined according to the procedure described in [16].

#### 2.4. Quantum chemical calculations

The geometries of the dye, radical cation and OH $\cdot$  adducts were optimised using the B3LYP/6-31G+ density functional theory (DFT) method [17, 18], which is available in the Gaussian 09 suite of programs [19]. Calculations of the excited states were performed using the time-dependent DFT (TD-DFT) method [20]. The ionisation potential ( $I_p$ ) of the dye was calculated from the difference in total energy between the neutral molecule and its radical cation at the optimised geometry of the neutral molecule. The  $E_{\text{HOMO}}$  molecular orbital energy and the electron density were determined using the AM1 method with HyperChem software [21] and/or the B3LYP/6-31G+ density functional theory (DFT) method.

### 3. RESULTS AND DISCUSSION

#### 3.1. Cyclic and differential pulse voltammograms of C. I. Acid Orange 52.

Preliminary information about the electrochemistry of C. I. Acid Orange 52 was obtained from the dependence of the current ( $i$ ) on the potential ( $E$ ). Both cyclic voltammetry (CV) and differential pulse voltammetry (DPV) were used in electrochemical oxidation at the platinum electrode. The latter method exhibits better resolution and enables better separation of the peaks. Examples of CV and DPV voltammograms of C. I. Acid Orange 52 are shown in Figure 2. The oxidation of this dye proceeded in at least two steps. The first peak is located at 0.71 V, and the second is located at 0.86 V. In the reverse scan, one poor current peak appeared, indicating the reduction of the products formed during oxidation of the dye.

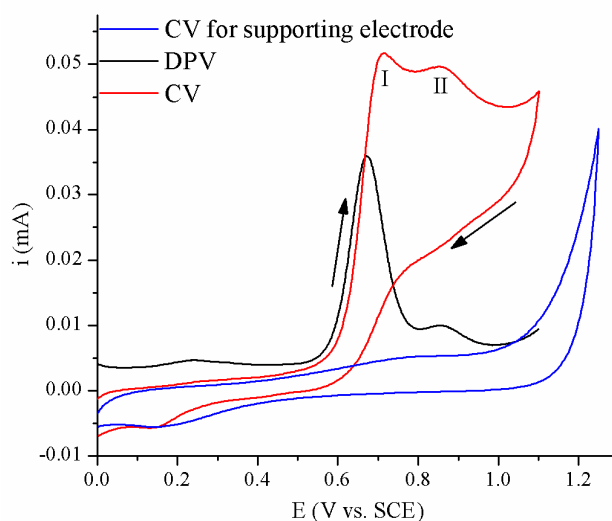


**Figure 2.** CV and DPV voltammograms of C. I. Acid Orange 52 oxidation at a platinum electrode;  $c=1\times 10^{-3}$  mol  $\text{dm}^{-3}$  in 0.1 mol  $\text{dm}^{-3}$   $\text{NaClO}_4$ ,  $v = 0.01$  V  $\text{s}^{-1}$ .

To estimate the characteristic of the electrode reaction, two approaches are usually applied: analyses of the peak current ( $i_p$ ) at different concentrations of the substrate relative to the square root of the scan rate ( $v^{1/2}$ ) (Figure 3A) and  $\ln(i_p)$  on  $(\ln v)$  (Figure 3B) [22]. Although Figure 3A shows good linearity of the peak current ( $i_p$ ) relative to the square root of the scan rate ( $v^{1/2}$ ), this curve does not cross the origin of the coordinates. This indicates that the process may be controlled either by diffusion or by adsorption. For a better explanation of this problem, the latter dependence was tested (Figure 3B). The slope of the curve of  $\ln(i_p)$  vs  $\ln(v)$  over the range of 0.38-0.44 apparently proved the diffusion-controlled nature of the process [23-25].

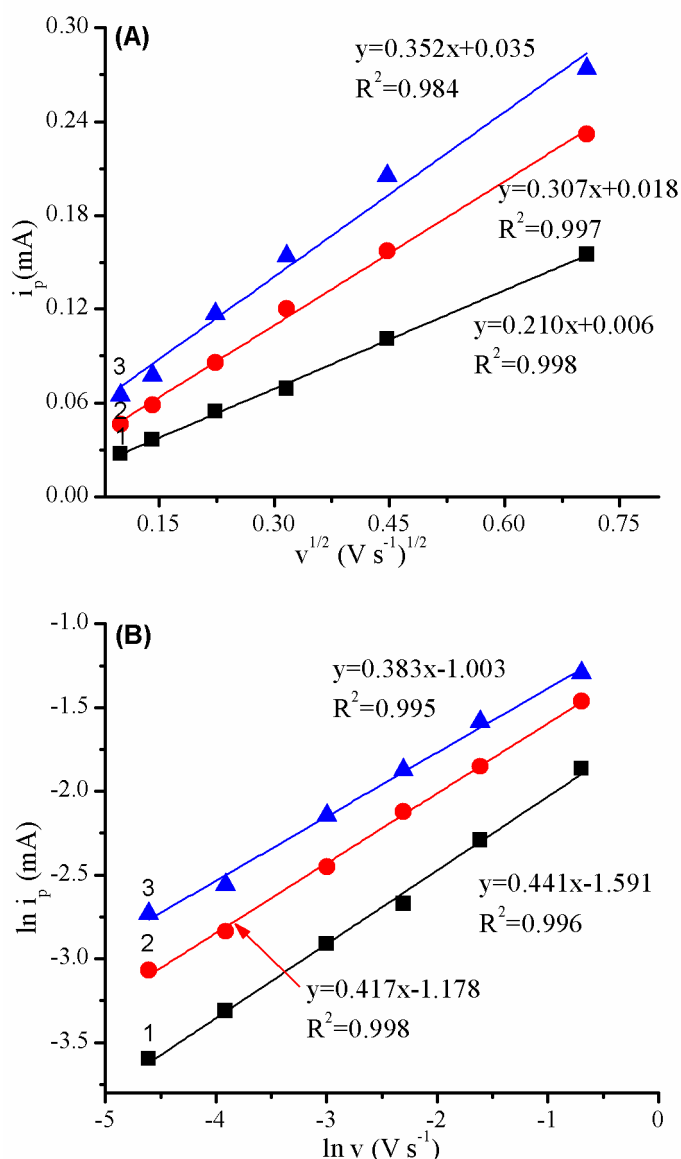


**Figure 3.** (A) Dependence of the anodic peak current ( $i_p$ ) on the square root of the scan rate ( $v^{1/2}$ ), (B) Dependence of  $\ln(i_p)$  on  $\ln(v)$  in oxidation at various concentrations of C. I. Acid Orange 52; 1:  $c=0.5$  mmol dm<sup>-3</sup>, 2:  $c=1.0$  mmol dm<sup>-3</sup>, 3:  $c=1.5$  mmol dm<sup>-3</sup> in 0.1 mol dm<sup>-3</sup> NaClO<sub>4</sub>.

To determine whether or not the studied electrode reaction is reversible, the effect of the scan rate ( $v$ ) on the potential ( $E_p$ ) of methyl orange electrooxidation was investigated (Figure 4A). It was

found that ( $E_p$ ) changed when the scan rate ( $v$ ) increased, confirming the irreversibility of the process. Therefore, the electron transfer coefficient ( $\beta n_\beta$ ) for dye electrooxidation was calculated using equation (4) [24, 26, 27].

$$E_p = \left( \frac{R \times T}{2 \times \beta n_\beta \times F} \right) \times \ln v + \text{const} \quad (4)$$

where  $E_p$  is the peak potential (V),  $R$  is the universal gas constant (8.314 J/mol K),  $F$  is the Faraday constant (96.478 C/mol),  $T$  is the temperature (298 K) and  $v$  is the scan rate ( $\text{Vs}^{-1}$ ). From a plot of  $E_p=f(\ln v)$  (Figure 4B), it was possible to determine the  $\beta n_\beta$  value, which depended on dye concentrations and equalled 0.58-0.74.

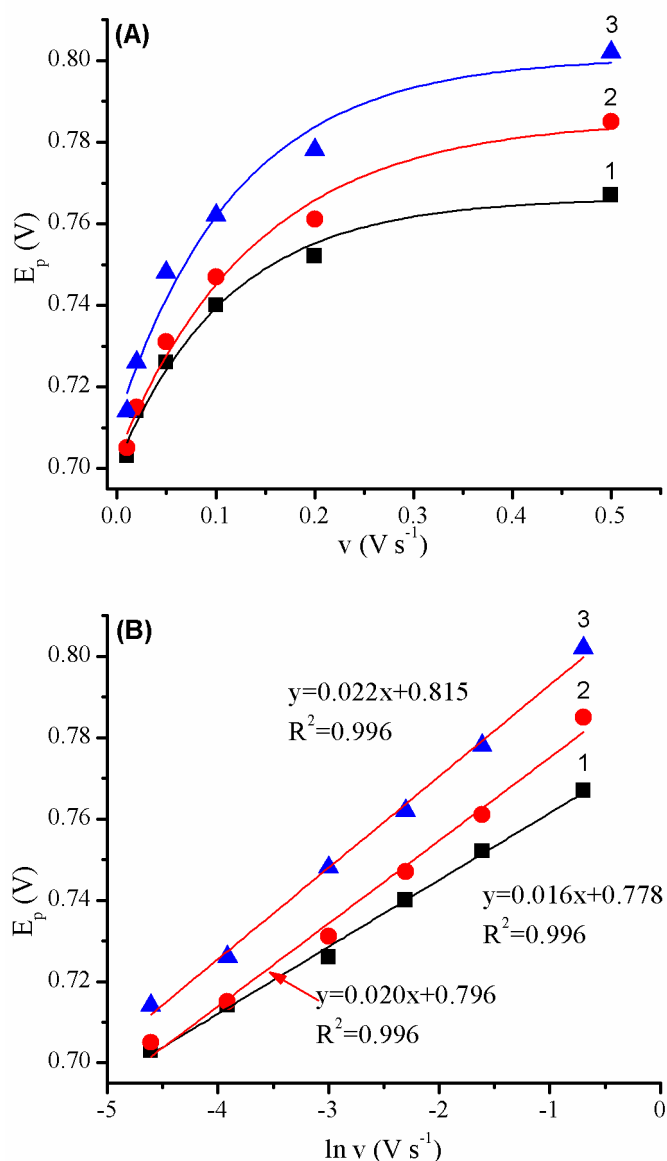


**Figure 4.** (A) Dependence of the anodic peak potential ( $E_p$ ) on the scan rate ( $v$ ) for the oxidation of C. I. Acid Orange 52 at platinum electrode, (B) Relationship between the anodic peak potential ( $E_p$ ) and the logarithm of the scan rate ( $\ln v$ ) for the first step of methyl orange oxidation; 1:  $c=0.5 \text{ mmol dm}^{-3}$ , 2:  $c=1.0 \text{ mmol dm}^{-3}$ , 3:  $c=1.5 \text{ mmol dm}^{-3}$  in  $0.1 \text{ mol dm}^{-3} \text{ NaClO}_4$ .

On the other hand, according to Bard and Faulkner [24], the  $\beta$  value may also be determined from equation (5). The calculated  $\beta$  value is  $0.65 \pm 0.2$ , indicating that in the first step of the dye electrooxidation, one electron is exchanged.

$$\beta = \frac{47.7}{E_p - E_{p/2}} \quad (5)$$

Finally, the influence of the dye concentration on its oxidation was also examined with the application of CV and DPV (Figure 5) at a platinum electrode. When the concentration of the dye increased, the current peak ( $i_p$ ) of the dye oxidation estimated by CV and DPV linearly increased, as illustrated by the equations shown in Figure 5.

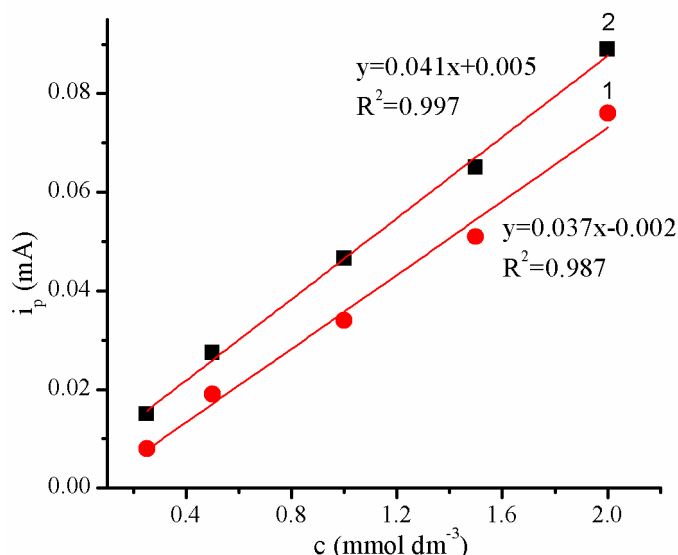


**Figure 5.** Dependence of the anodic peak current ( $i_p$ ) in C. I. Acid Orange 52 oxidation on the dye concentration (1. CV; 2 DPV) at the platinum electrode.

This linear dependence of the anodic peak current ( $i_p$ ) on the dye concentration ( $c$ ) enables its quantification in various samples using CV and DPV techniques.

In the final part of the electrochemical study of C. I. Acid Orange 52 oxidation, due to the expected synergy effect [5], titanium electrodes coated with TiO<sub>2</sub> (70%)/RuO<sub>2</sub> (30%) and TiO<sub>2</sub> (97%)/RuO<sub>2</sub> (3%) were tested. These electrodes have larger specific surface areas than platinum electrodes with the same geometry. Examples of C. I. Acid Orange 52 oxidation carried out with the application of different electrode materials are presented in Figure 6.

The oxidation of the dye at platinum occurred in two irreversible steps, whereas at Ti/TiO<sub>2</sub>/RuO<sub>2</sub> electrodes, the process proceeded in one step before the potential reached the value at which oxygen evolution began. The current of the first oxidation step depended on the electrode used, being the lowest at the platinum electrode and the highest at the titanium electrode coated with TiO<sub>2</sub> (70%)/RuO<sub>2</sub> (30%). To estimate the character of the electrode reaction, the dependence of  $\ln(i_p)$  of C. I. Acid Orange 52 oxidation vs  $\ln(v)$  was determined (Figure 7). The slope values indicated that the process is diffusion-controlled [23-27].

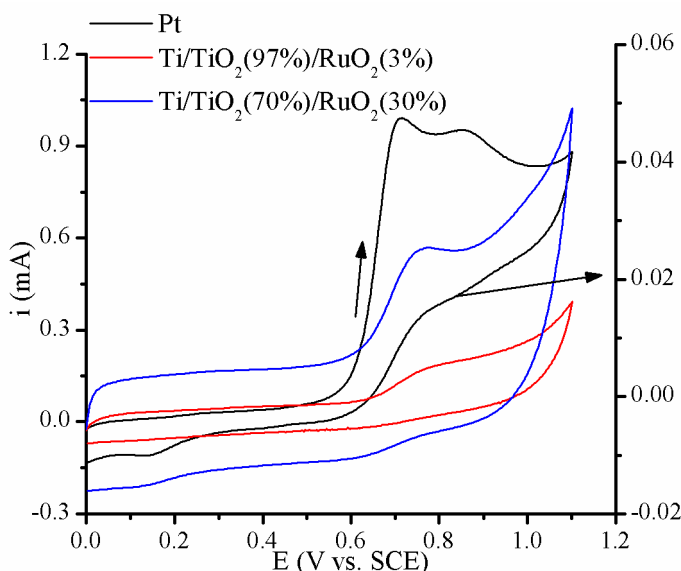


**Figure 6.** Cyclic voltammograms of C. I. Acid Orange 52 recorded at different electrode materials;  $c=1.0 \text{ mmol dm}^{-3}$  in  $0.1 \text{ mol dm}^{-3} \text{ NaClO}_4$ ,  $v=0.01 \text{ Vs}^{-1}$ .

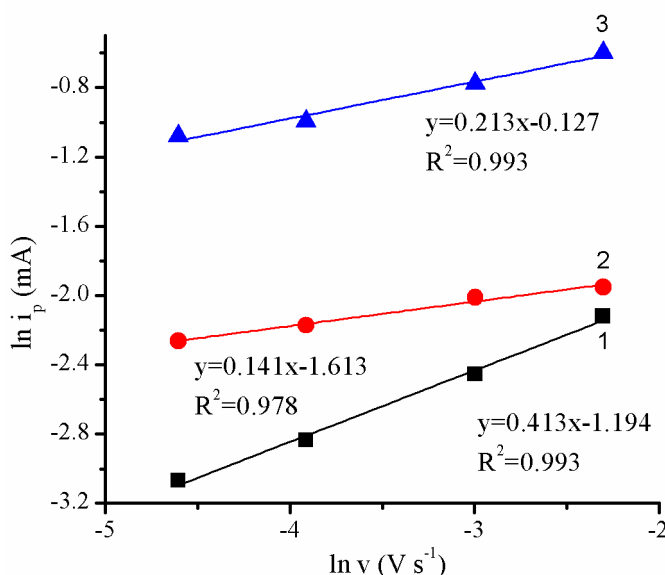


**Figure 7.** Dependence of  $\ln(i_p)$  on  $\ln(v)$  for C. I. Acid Orange 52 oxidation recorded at different electrode materials; 1: Pt, 2: Ti/TiO<sub>2</sub> (97%)/RuO<sub>2</sub> (3%), 3: Ti/TiO<sub>2</sub> (70%)/RuO<sub>2</sub>(30%).

**Table 1.** Half-wave potential ( $E_{1/2}$ ), peak current ( $i_p$ ), anodic transition coefficient ( $\beta_{n\beta}$ ) and heterogeneous rate constant ( $k_{bh}$ ) values for the first step of C. I. Acid Orange 52 oxidation;  $c = 1.0 \text{ mmol dm}^{-3}$  in  $0.1 \text{ mol dm}^{-3} \text{ NaClO}_4$

Electrode	$E_{1/2}$ (V)	$i_p \times 10^4$ (A)	$\beta_{n\beta}$	$k_{bh} \times 10^4$ ( $\text{cm s}^{-1}$ )
Pt	0.698	0.46	0.84	2.64
Ti/TiO <sub>2</sub> (97%)/RuO <sub>2</sub> (3%)	0.739	1.04	0.76	2.38
Ti/TiO <sub>2</sub> (70%)/RuO <sub>2</sub> (30%)	0.745	3.40	0.68	3.21

The overall results regarding the electrochemistry of C. I. Acid Orange 52 at different electrode materials are summarised in Table 1.

These results indicate that the oxidation of the dye proceeded more easily at the platinum electrode. However, because the peak current ( $i_p$ ) at the electrode coated with  $\text{TiO}_2/\text{RuO}_2$  (70%/30%) was the highest, in further photoelectrochemical experiments, only this electrode was used.

### 3.2. Electrochemical (electrolysis) and photoelectrochemical (photoelectrolysis) treatment of C. I. Acid Orange 52

In the next step, following a procedure similar to that adopted previously [28], electrolysis of the tested dyes was carried out using the conditions corresponding to a current density of  $2.0 \times 10^{-2} \text{ A cm}^{-2}$ . During preliminary investigation, it was found that favourable substrate conversion calculated as a change in the absorbance was achieved when the electrolysis was carried out within 1.5 h at room temperature. To improve the yield of C. I. Acid Orange 52 conversion, a combined electrochemical (with the application of the titanium electrode coated with a mixture of  $\text{TiO}_2$  and  $\text{RuO}_2$ ) and photochemical processes were conducted using the parameters applied in a single electrochemical process. The results of these experiments, including UV-induced dye degradation, are shown in Table 2. It is evident that a single electrochemical oxidation of C. I. Acid Orange 52 resulted in approximately 83% decolourisation after 1.5 h treatment, whereas the substrate was only partly decolourised (49%) by the influence of 254 nm light within the same time. However, when a combined procedure with the use of 254 nm light was applied, the conversion of the dye was almost complete (97.2%). This study also showed that the conversion of MO estimated as a change in TOC and COD strongly depended on the experimental conditions.

**Table 2.** Dependence of C. I. Acid Orange 52 degradation on the type of process

Process type	MO conversion $\eta_{\text{TOC}}$ (%) <sup>a</sup>	MO conversion $\eta_{\text{COD}}$ (%) <sup>b</sup>	MO conversion $\eta_{\text{Abs}}$ (%) <sup>c</sup>
Electrolysis	18.0	23.2	83.2
UV irradiation (254 nm)	4.1	11.2	49.1
UV irradiation (300 nm)	2.3	6.5	2.1
Photoelectrochemical treatment (254 nm)	31.9	35.2	97.2
Photoelectrochemical treatment (300 nm)	31.4	34.9	85.8

The simple electrochemical treatment of MO resulted in approximately 18% TOC and 23% COD removal, whereas irradiation with 300 nm and 254 nm light caused only approximately 2-4% and 6-11% conversion of the dye based on TOC and COD removal, respectively. However, when the combined procedure with the application of 254 nm and 300 nm light was applied, the conversion of the dye increased to approximately 32% and 35% in terms of  $\eta_{\text{TOC}}$  and  $\eta_{\text{COD}}$ , respectively.

The concentration of the dye was  $0.04 \text{ mmol dm}^{-3}$ ; the initial pH was 7.0; the current density was  $2.0 \times 10^{-2} \text{ cm}^{-2}$ ; the temperature was  $20 \text{ }^\circ\text{C}$ ; the electrolysis, photolysis and photoassisted

electrolysis duration was 1.5 h; the electrolyte was  $0.1 \text{ mol dm}^{-3} \text{ NaClO}_4$ ; the volume of the solution was 100 ml; and the <sup>a, b, c</sup>conversion of the dye was presented as a change in TOC ( $\eta_{\text{TOC}}$ ), COD ( $\eta_{\text{COD}}$ ) and absorbance ( $\eta_{\text{Abs}}$ ).

### 3.3. Suggested mechanisms of C. I. Acid Orange 52 oxidation

As mentioned in the Introduction, the electrochemical oxidation of organic compounds may be achieved by direct anode oxidation and/or by indirect oxidation with hydroxyl radicals,  $\text{OH}^\cdot$ , generated at the anode.

Although the intermediate products of C. I. Acid Orange 52 electrodegradation were reported in the literature previously [8], in this paper, an attempt was made to propose the initial product(s) formed, confirmed by quantum chemical calculations. The first approach refers to the distribution of electron density in the molecule (Figure 8, 9), which determines the ease of electron release.

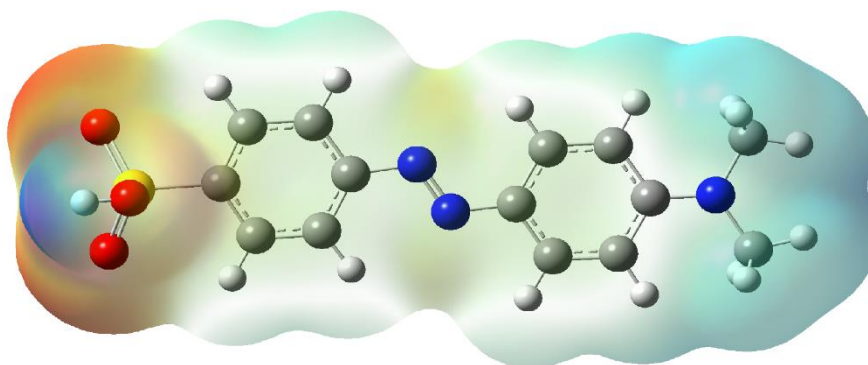


**Figure 8.** The electron density of C. I. Acid Orange 52 (B3LYP/6-31G+ density functional theory).

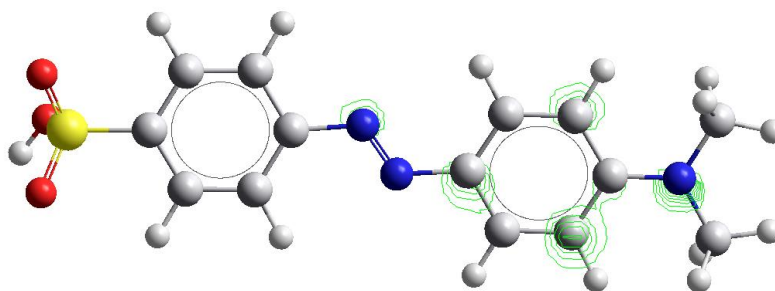


**Figure 9.** The electron density of C. I. Acid Orange 52 (the AM1 method with HyperChem software).

It is evident that independently of the calculation methods, the highest electron density was found on the nitrogen of the N,N-dimethylamino group, and slightly lower electron density was found on the phenyl ring belonging to the coupling component of the dye. Additionally, Figure 9 also shows slightly higher electron density on the azo linkage nitrogen. All these data indicate that these sites might be easily oxidised. According to the literature [28], the N,N-dimethylamino group is highly electron rich, making it the most susceptible to one-electron transfer. This results in cation radical formation (Figure 10), which might be the initial step of dye oxidation.

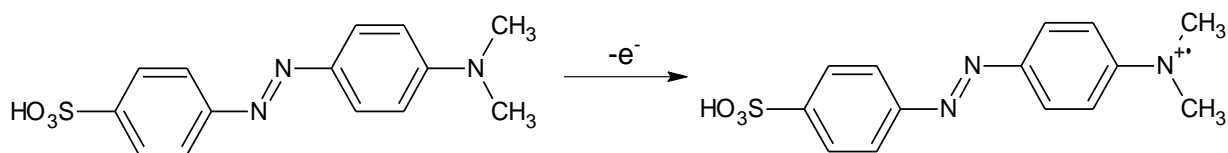
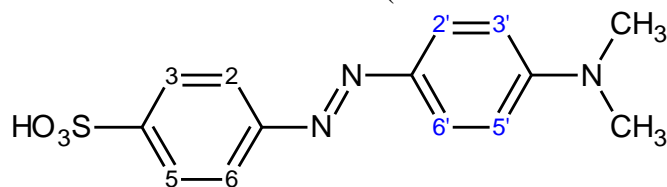


**Figure 10.** The scheme of radical cation formation.

The calculated ionisation potential ( $I_p$ ) was found to be 6.5117 eV (B3LYP/6-31G+ density functional theory), and the  $E_{\text{HOMO}}$  was -8.5692 eV (AM1 method with HyperChem software).

Alternative mechanisms involving the formation of an  $\text{OH}\cdot$  adduct to the benzene rings or to an azo group as the initial step of dye degradation were also considered [30]. Quantum chemical calculations of the optimised radical structures showed that possibly the adduct substituted with hydroxyl radical in position 2 (Table 3), having the lowest energy, is the most likely intermediate that could be formed. It is worth mentioning that other adducts of the dye with  $\text{OH}\cdot$  radicals were not formed. Therefore, all of these data shown above clearly indicate that the process of dye degradation might be very complex.

**Table 3.** The results of quantum chemical calculations (B3LYP/G-31G+ density functional theory)\*



The position of $\text{OH}\cdot$	Energy [a.u.]	Energy [eV]	$\Delta E$
none	-1330.099	-36193.324	-
2	-1405.894	-38255.781	0
3	-1405.878	-38255.346	0.016
3'	-1405.884	-38255.510	0.010

\*The other adducts are not formed.

#### 4. CONCLUSIONS

Electrolysis of C. I. Acid Orange 52 was performed at Pt and Ti/TiO<sub>2</sub>/RuO<sub>2</sub> electrodes. The oxidation of the dye at Pt occurred in two irreversible steps, whereas at Ti/TiO<sub>2</sub>/RuO<sub>2</sub> electrodes, the process proceeded in one step before the potential reached the value at which oxygen evolution began. Both processes were diffusion-controlled. Although the oxidation of the dye at the platinum electrode proceeded at a lower  $E_{1/2}$ , the peak current ( $i_p$ ) and heterogeneous rate constant ( $k_{bh}$ ) for the first step of degradation were higher when the Ti/TiO<sub>2</sub>/RuO<sub>2</sub> electrodes were used. During photosupported (254 nm and 300 nm) electrolysis, a synergistic effect was observed in terms of absorption, COD and TOC changes. Based on quantum chemical calculations, the primary degradation products of electrooxidation were proposed.

## References

1. E. Korduli, K. Bourikas, A. Lycourghiotis and C. Kordulis, *Catal. Today*, 252 (2015) 128.
2. M. Nawaz, W. Miran, J. Jang and S.E. Lee, *Catal. Today*, 282 (2017) 38.
3. J.A. Allen, K.Y.H. Khader and M. Bino, *J. Chem. Technol. Biotechnol.*, 62 (1995) 111.
4. K. Rajeshwar, J.G. Ibanez and G.M. Swain, *J. Appl. Electrochem.*, 24 (1994) 1077.
5. R. Pelegrini, P. Peralta-Zamora, A.R. Andrade, J. Reyes and N. Duran, *Appl. Catal., B*, 22 (1999) 83.
6. S. Ardizzone and S. Trassati, *Adv. Colloid Interface Sci.*, 64 (1996) 173.
7. S. Li, Y. Zhao, J. Chu, W. Li and H. Yu G. Liu, *Electrochim. Acta*, 92 (2013) 93.
8. E. Isarain - Chaves, M.D. Baró, E. Rossinyol, U. Morales - Ortiz, J. Sort, E. Brillas and E. Pellicer, *Electrochim. Acta*, 244 (2017)199.
9. S.V. Mohite, V.V. Ganbawle and K.Y. Rajpure, *J. Energy Chem.*, 26 (2017) 440.
10. E. Brillas and C.A. Martinez-Huitle, *Appl. Catal. B: Environ.*, 166-167 (2015) 606.
11. F.C. Moreira, R.A.R. Boaventura, E.Brillas and V.J.P. Vilar, *Appl. Catal. B*, 202 (2017) 217.
12. F.C. Moreira, S. Garcia-Segura, V.J.P. Vilar, R.A.R. Boaventura and E. Brillas, *Appl. Catal. B*, 142 (2013) 877.
13. E. Isarain-Chaves, R.M. Rodriguez, P.L. Cabot, F. Centellas, C. Arias, J.A. Garido and E. Brillas, *Electrochim. Acta*,56 (2010) 215.
14. M. Seralathan, R.A. Osteryong and J.G. Osteryong, *J. Electroanal. Chem. and Interfacial Electrochem.*, 222 (1987) 69.
15. Z. Galus, *Fundamentals of electrochemical analysis*. Harwood & PWN; 1994, pp. 242, 284.
16. W. Hermanowicz, J. Dojlido, W. Dozanska, B. Koziorowski and J. Zerbe, *Fizyczno-chemiczne badanie wody i ścieków*, Arkady, Warszawa 1999, pp. 93, 333, 421.
17. A.D. Becke, *J. Chem. Phys.*, 98 (1993) 5648.
18. C. Lee, W Yang and R.G. Parr, *Phys. Rev. B*, 37 (1988) 785.
19. M.J. Frisch, G.W. Trucks, H.B. Schlegel, G.E. Scuseria, M.A. Robb, J.R. Cheeseman, G. Scalmani, V. Barone, B. Mennucci and G.A. Petersson, *Gaussian 09*; Gaussian Inc.:Wallingford, CT, 2009.
20. R. Bauernschmitt and R. Ahlrichs, *Chem. Phys. Lett.*, 256 (1996) 454.
21. HyperChem Release 7 for Windows, *Hypercube, Inc.* (2002).
22. M.Y. Wang, D. Zhang, Z.W. Tong, X.Y. Xu and X.J. Yang, *J. Appl. Electrochem.*, 41 (2011) 189.
23. A.K. Timbola, C.D. Souza, C. Soldi, M.G. Pizzolatti and A. Spinelli, *J. Appl. Electrochem.*, 37 (2007) 617.
24. A.J. Bard and L.R. Faulkner, *Electrochemical Methods, Fundamentals and Applications*. 2nd ed. John Wiley & Sons, New York, 2001, pp. 236, 503, 709.
25. C.M.A. Brett and A.M.O. Brett, *Electrochemistry: Principles, Methods, and Applications*. Oxford University Press, New York, 1993, pp. 427.
26. J.A. Harrison and Z.A. Khan, *J. Electroanal. Chem. and Interfacial Electrochem.*, 28 (1970) 131.
27. R.S. Nicholson and I. Shain, *Anal. Chem.*, 336 (1964) 706.
28. R. Sałata, K. Siwińska-Stefańska and J. Sokołowska, *Int. J. Electrochem. Sci.*, 14 (2019) 792.
29. S. Padmaja and S. Madison, *J. Phys. Org. Chem.*, 12 (1999) 221.
30. S.H. Liu, S.L. Wang, X.Y. Sun, W. Z. Li, Y.M. Ni, W.F. Wang, M. Wang and S.D. Yao, *Acta Chim. Sinica*, 62 (2008) 818.